UNIVERSITY OF CALIFORNIA,
IRVINE

Magnetic Iron Oxide Nanoparticles and a Polydiacetylene Coating to Create a Biocompatible and Stable Molecule for Use in Cancer Diagnostics and Early detection in Molecular Medicine

THESIS

submitted in partial satisfaction of the requirements
for the degree of

MASTER OF SCIENCE

in Biomedical Engineering

by

Shweta Bhatnagar

Thesis Committee:
Assistant Professor Jered Haun, Chair
Associate Professor Gultekin Gulsen
Assistant Professor Chang Liu

2017

DEDICATION

To

my parents and friends

in recognition of their time, love, and help.

Table of Contents

LIST OF FIGURES v

ACKNOWLEDGMENTS vi

ABSTRACT OF THE THESIS: vii

CHAPTER 1: INTRODUCTION AND BACKGROUND 1

Cancer and Statistics: 1

Diagnosing Cancer and Tests: 2

Different Treatments of Cancer: 3

Nanotechnology and Nanomedicine: 4

Magnetic Nanoparticle Signals and MRI detection: 5

Synthesis of Iron Oxide Nanoparticles: 7

Use of Nanotechnology in Cancer Diagnosis Through Polymer Encapsulation: 9

Targeting Cancer Cells with MNPs: 12

Summary of the Advantages of MNPs in Cancer Treatment: 13

Study of Using Bioorthogonal Chemistry and Bonding for Cancer Detection: 14

CHAPTER 2: METHOD HISTORY AND EXPERIMENTS DONE IN THE PAST 18

Initial Concept of Self-Assembly of Phospholipid – PEG Coating through Dual Solvent Exchange: 18

Use of Polydiacetylenes for Iron Oxide Cores: 20

Process of PEGylation after PDA coating: 24

Quantification of Iron Oxide Nanocrystals: 26

Measurements Using DLS and Nanodrop: 27

Past Work From a Previous Student 28

CHAPTER 3: METHOD 30

Project Overview: 30

Coating Method, Ferrozine Assay, and PEGylation Process: 30

CHAPTER 4: RESULTS AND DISCUSSION 39

CHAPTER 5: CONCLUSION AND FUTURE DIRECTIONS 45

REFERENCES: 46

APPENDIX: 49

CALCULATIONS: 52

LIST OF FIGURES

Figure 1: Biocompatible coating around iron core [7] 7

Figure 2: Formation of Monodisperse Iron Oxide Nanoparticles [10] 8

Figure 3: Multilayer concept for magnetic nanoparticle [4] 10

Figure 4: Two images of BOND Between TCO Modified Antibody and Tz Nanoparticle [6],[14] 15

Figure 5: Difference Between BOND 1 and BOND 2 [14] 16

Figure 6: Flow diagram of Process to Therapeutics 17

Figure 7: Film Hydration Method vs. Solvent Exchange Method [8] 20

Figure 8: Colorimetric Properties of PDA [16], [17], [18] 22

Figure 9: PDA coating around Iron Oxide Cores [16] 23

Figure 10: PCDA Chemical Formula and Structure, HCDA Chemical Formula [20], [21] 24

Figure 11: PDA Structure with Primary Antibody [17] 24

Figure 12: Carbomiide Reaction Using Coupling Reagents [23] 26

Figure 13: Structure of Ferrozine [24] 26

Figure 14: Sizing of Purchased 10 nm cores with HCDA Samples 40

Figure 15: Sizing of Purchased 20 nm cores with HCDA Samples 41

Figure 16: Sizing of Purchased 20 nm cores with PCDA 42

ACKNOWLEDGMENTS

I would like to express many thanks and all my appreciation to my committee chair, Professor Jered Haun, who was always there to guide me in this project throughout my graduate school career. With his inspiration and passion for research, I was able to gain a lot of knowledge from him and my team members throughout the two years. Dr. Haun has always been a role model and I am so thankful for working with him and making these two years memorable and full of different experiences.

I would like to thank my committee members, Professor Gultekin Gulsen and Professor Chang Liu, for being a part of my team and reviewing my thesis.

In addition, I would like to thank the Haun lab team for being a family to me and a second home for me. I would like to express my gratitude for everyone who has always been there for me, academically, professionally, or socially.

I want to thank all the former students who have also guided and mentored me in this project throughout.

ABSTRACT OF THE THESIS:

Magnetic Iron Oxide Nanoparticles and a Polydiacetylene Coating to Create a Biocompatible and Stable Molecule for Use in Cancer Diagnostics and Early detection in Molecular Medicine

By

Shweta Bhatnagar

Master of Science in Biomedical Engineering

University of California, Irvine, 2017

Professor Jered Haun, Chair

Earlier cancer detection and diagnosis is essential to prevent cancer mortality in nanomedicine and nanotechnology. Fluorescence and magnetic signals provide a way for earlier detection through imaging systems. Magnetic iron oxide nanoparticles have a superparamagnetism feature that allows them to act as contrast agents that can be detected through a magnetic resonance imaging system. These iron oxide cores have a polymer coating around them to provide stability, prevent aggregation, and allow for biocompatibility within the body. In addition, these functional coatings can have ligands and peptides for detection and therapy purposes. One functional coating is a polydiacetylene coating due to its chromatic and optical properties. When polymerized, it has the ability to change color in the visible spectrum to blue (not a fluorescent signal) and when heated, it changes to a red color (fluorescent signal). This way a strong and stable layer is formed around the iron oxide cores. These coatings are placed on the iron cores using a modified dual solvent exchange method, in which DMSO is slowly replaced by water without the use of organic solvents previous used. In addition, these nanoparticles can then be PEGylated, which provides a

more stable and water soluble compound in aqueous solutions. Measurements can be taken through dynamic light scattering for size distributions and zeta potential and the Nanodrop for absorbance. Ideal sizes are about 30 nm for MNPs. Moreover, for future directions, there can be more molecules attached to the coated layers to use for molecular detection and analysis.

CHAPTER 1: INTRODUCTION AND BACKGROUND

Cancer and Statistics:

Cancer is one of the major diseases in the United States and around the world [1]. Typically, the cells in the body have a process of growth, division, and death. New cells are created by the body when old cells die. However, at times, when this process does not go correctly, new cells can be created unnecessarily, without death of the older cells. In these abnormal growth conditions of cells, a clump forms that is called a tumor, which can be of two types, either benign or malignant, and can spread around the body and damage healthy tissues. Malignant tumors, which are more dangerous and are cancerous, can form when these tumors spread to other parts of the body, which is the process of metastasis, from the original location. On the other hand, benign tumors, which are noncancerous, don't spread to the rest of the body [2],[3]. There are different types of cancers, such as breast cancer, lung and bronchus cancer, mouth cancer, esophagus cancer, colon cancer, ovarian cancer, rectal cancer, bladder cancer, skin cancer, thyroid cancer, kidney cancer, pancreatic cancer and many more [1],[2],[3]. The average number of deaths that occur amongst the population is 171.2 per 100,000 people per year, according to National Cancer Institute. Also, the number of cases that arise per 100,000 people is 454.8 per year. Cancer deaths are higher in men than in women with a comparison of 207.9 per 100,000 men versus 145.4 per 100,000 women. African American men have the highest death rate from cancer, which is about 261.5 per 100,000. Death rate is lowest in Asian/Pacific Islander women, which is about 91.2 per 100,000. About 60-70% of cases occur in Africa, Asia, and Central and South America [1].

There are many factors that can affect cancer, such as tobacco use and cigarette smoking, food diet and exercise, work environment, age, and any family history of cancer. Tobacco use can cause lung damage and lung cancer. Cigarette smoking can easily cause cancer in the lungs, mouth, esophagus, or larynx. Also, the more fat intake in food and diet, the higher the risk of cancer. Certain ethnicities and races can have a higher risk of cancer, as mentioned above for African Americans. Risks of cancer also increase if an immediate family member has been exposed to cancer. The work environment can also affect cancer if one is working with chemicals or vapors that can be inhaled. Moreover, being exposed to the sun can lead to cancer, such as skin cancer [3]. As can be seen from above, there are multiple factors that can lead to the different types of cancers that form in the body.

Diagnosing Cancer and Tests:

Various tests could help diagnose cancer. As women get older, the risk of breast cancer also increases. Doctors can diagnose this cancer earlier by using a clinical breast exam, in which a doctor physically checks the breasts for any knots or lumps. A mammogram, which uses X-ray analysis of the breasts, is also used for detection of breast cancer. It is recommended that women between the ages of 50 and 75 should have this done every two years since cancer risk might increase during that time. To diagnose cervical cancer, a Pap smear method is used in which the doctor has some extracted cells from the cervix to be tested. On the other side, males are at a risk of prostate cancer. To diagnose this cancer, a prostate-specific antigen (PSA) test is used. Patients with this cancer typically have high amounts of PSA in their blood, but this could also be a result from an infection. More tests would be needed to be performed in order to determine what cancer it is. Various tests exist in order to determine the stage and type of cancer [3].

Different Treatments of Cancer:

Cancer can be treated if it hasn't spread in the body or if the tumor is still of a small size. For this reason, early cancer detection is beneficial in possibly eradicating the tumor from spreading and becoming bigger in the body. There are various ways to treat cancer, such as surgery, radiotherapy, and chemotherapy. Surgery can be performed for some patients whose cancer is malignant, but hasn't spread to other parts of the body. Surgeries cannot be performed in patients where the surgery would possibly damage one of the major organs, such as brain or liver. Different types of surgeries include laser, laparoscopic, Moh's surgery, and cryosurgery. In laser surgery, optical properties of light and heat from lasers are used to burn up the tumor cells and destroy them. In laparoscopic surgery, doctors can see inside the body with a camera and use a surgical tool to remove the cancer cells. In Moh's surgery, layers of the diseased cells are removed, leaving the layer of healthy cells and tissue intact and undamaged. In cryosurgery, the cancer cells are frozen with products, such as liquid nitrogen, in order to destroy these cells. In radiotherapy, the use of radiation, such as X-rays or gamma rays, can help destroy the cancer cells. However, this radiation can spread to healthy cells as well and damage healthy tissue. In chemotherapy, cytotoxic medications are used to destroy cells that have spread throughout the body [3],[4]. This method can be used as a combination with surgery or radiation. There are other types of treatments as well. Immunotherapy focuses on making the body create more immune cells, such as white blood cells, called lymphocytes. Two types of lymphocytes include B-cells and killer T cells, which can help protect the body and attack the cancer cells. Surgery, radiation therapy, or chemotherapy can be used in addition to this method. Moreover, in hormone therapy, the patient uses drugs that have hormones that can reduce the effect of other hormones, such as

estrogen and testosterone, to treat breast and prostate cancer. Since increased levels of estrogen can make breast cancer cells grow faster and testosterone levels can make prostate cancer cells grow, limiting these hormone levels with drugs would help in limiting the growth of these cancer cells. Also, removing the ovaries or testicles can also lead to a reduction of those hormones. As seen from above, there are various treatments and technologies to eliminate or reduce the effect of different types of cancer [3].

Nanotechnology and Nanomedicine:

Early detection and molecular analysis of cancer cells is essential in preventing the disease from spreading further throughout the body. Functional molecules in these types of cells are not able to work properly and thus, early analysis, detection, and diagnosis of these in molecular medicine is beneficial. Cancer cells multiply very quickly and can invade the body very quickly because of their behavior and the ability to change so drastically. Tumors grow and change rapidly within a short amount of time. Moreover, some cancers are very difficult to discern with screening. Thus, there is a need to analyze them as quickly as possible. Death from cancer could be prevented through early diagnosis, detection, and therapy and treatment of cancerous cells [5]. Current methods for detection consist of Western blotting, flow cytometry, and immunofluorescence imaging are not the best methods since they require a large number of cells and cannot provide sufficient amount of information about the location of tumors [6]. In contrast, nanoimaging and signals from nanomaterials, such as iron oxide magnetic particles, fluorescent materials, such as gold nanoparticles or quantum dots, could be useful in molecular diagnostics and detection since visualization of the affected area is possible. This imaging allows doctors to know the

location of the cancer cells, see how cancer cells behave with therapy, and see the expression and activity of molecules that affect these cancer cells [4].

There are two main types of nanoimaging: fluorescence imaging and Magnetic Resonance Imaging (MRI). According to *Gobbo et. al,* quantum dots, which are nanocrystals, are used as fluorescence methods of imaging. These nanocrystals help visualize the cancerous tissue by exciting them with a long wavelength and capturing images with a camera. Gold nanoparticles and quantum dots are able to detect multiple cancer biomarkers in blood assays and or biopsies. However, these nanoparticles are not compatible with imaging in vivo studies [4]. Magnetic nanoparticles (MNPs) consisting of superparamagnetic iron oxide (SPION) could be used for this early detection using a MRI system in vivo [4], [5].

Magnetic Nanoparticle Signals and MRI detection:

Since cancer is deadly and the symptoms usually start appearing late, survival is mostly plausible with early detection. Chemotherapy and radiotherapy are the most common treatments for cancer, but they are not specific to any type of tumor cells. Moreover, chemotherapy is expensive and can also affect healthy tissues with the cytotoxic agents. MNPs in addition to MRI imaging is a potential method for biomedicine and nanotechnology. That creates an issue for detection and thus, nanotechnology is used for cellular and molecular targeting with noninvasive methods to optimize selectivity in detection of cancer cells and thus, preventing high toxicity levels in the body. According to *Gobbo et. al* in a review paper, these particles could be made of cobalt, nickel, or iron [4], [7]. Iron oxide nanoparticles, typically the size of 10-100 nm in size, are used for detection since they are most biocompatible amongst the other magnetic elements and biodegradable, unlike gadolinium (Gd), which is toxic in the body [7]. MRI is a technique in which magnetic fields

applied to change the dipoles and moments of endogenous nuclei. A static field is applied to disturb the steady-state equilibrium in terms of time and space. After the magnetic field is removed, the nuclei are able to relax with two codependent relaxation times: T1 (spin-lattice relation) and T2 (spin-spin relaxation) [4]. These nanoparticles consist of a superparamagnetic iron core, which can be used as a T2 contrast agent for MRI signaling, according to *Yigit et. al* in a review paper [7]. It is seen that these magnetic particles affect the transverse relaxation time of protons in the nearby tissues and as a result, decrease the relaxation time reading, which the MRI can detect efficiently. In other words, these superparamagnetic properties allow nearby water molecules to change their spin-spin relaxation time, which can then help in seeing the expression of proteins and detecting tumors. This can then help in creating images that can help in extracting unhealthy and damaged tissues from the healthy tissues [4]. In addition to unlimited penetration through tissue, the MRI also provides a high tissue resolution and the use of these particles allows for higher sensitivity while detecting than other methods. The change in the readings can provide image contrasts and darkened tissues in order to detect the cancer signals efficiently and provide and deliver an image of this on the MRI system [7]. Therefore, these MNPs are able to provide a way for in vivo imaging of cancer in humans in addition to drug delivery, as therapeutic agents, which will be described in detail later. MNPs provide the most advanced method in research and development, as compared to the other nanoparticles, to provide imaging as well as therapy of cancer cells [4].

According to the review paper, these MNPs have a polymer coating around them to prevent agglomeration and oxidation during the synthesis process. It acts as a mediator between the iron core and specific biological molecules that can be targeted. Specifically, the

coating allows for targeting of macromolecules, such as peptides or functional nucleic acids, which can then be used to bind to surface antigens of desired cells via attachment of antibodies to the coating. Moreover, the coating can be used as a tag for imaging, using a functional group to attach near infrared fluorescent dyes to the polymer coating for in vivo and ex vivo imaging. Figure 1 below shows the magnetic nanoparticle with different attachments and functional groups around it, such as targeting peptides or targeting ligands. (a). It also shows that under an external magnetic field, the cores become magnetized and line up in one direction (b) [7].

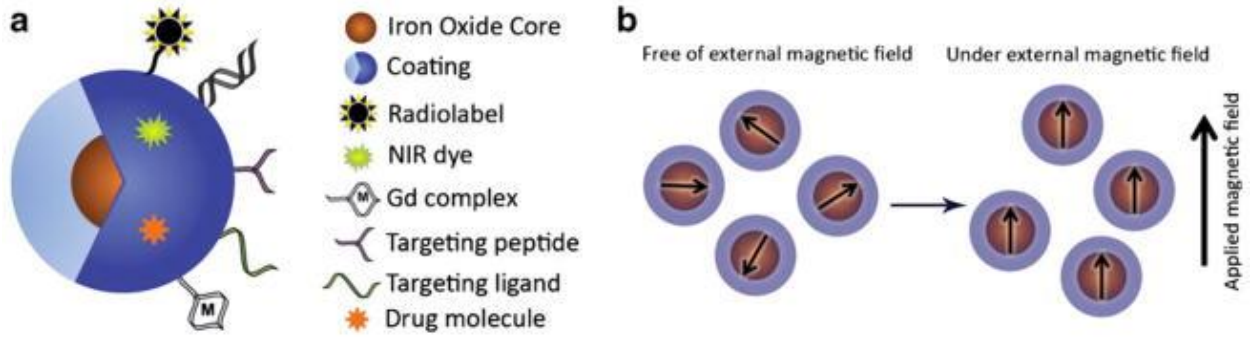

Figure 1: Biocompatible coating around iron core [7]

Synthesis of Iron Oxide Nanoparticles:

Iron oxide cores are synthesized by coprecipitation of Fe^{2+} and Fe^{3+} salts instead of cobalt or nickel since iron is less toxic according to *Yigit et. al* in the review paper. The cores are made of either magnetite (Fe_3O_4), maghemite (γ-Fe_2O_3), or a combination of them. Sizing of these cores are dependent on the salts used, the ratio of the two salts, pH and ionic bonds. These cores can have different sizes and have different surface modifications. It is essential to have this synthesis process under inert gases, such as argon and nitrogen, in order to prevent changes in the magnetic properties of the iron cores. Another method of how these nanocrystals are made is from thermal decomposition of precursor molecules in organic

solvents, such as toluene or hexane. They are made as a colloid with hydrophobic surfactants in nonpolar solvents, according to *Sheng Tong et. al*. These methods can lead to better size distributions of the cores [8], [9]. The synthesis process starts off with a one-pot reaction of iron (III) acetylacetonate, or $Fe(acac)_3$, with 1,2-alkanediol, oleic acid, and oleylamine in an organic solvent with high temperatures. The sizes of these particles are about 4-15 nm and depend on the surfactant used, surfactant-to-metal ratio, and concentration of the metal used [10]. Figure 2 below portrays this. First, all the components are heated to 200 degrees Celsius and then reflux occurs after two hours when the temperature is changed to 265 degrees Celsius [10].

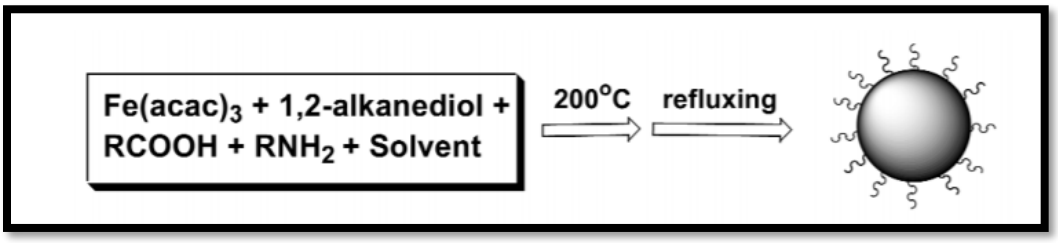

Figure 2: Formation of Monodisperse Iron Oxide Nanoparticles [10]

Magnetite has an oxygen atom in a face-centered cubic structure and Fe atoms in the tetrahedral and octahedral sites [11]. Surfactants or synthetic and natural polymers, such as polyethylene glycol (PEG), dextran polypeptides, chitosan, fatty acids, or gelatin are used as coatings around the iron cores to prevent agglomeration, provide stability, and attach functional groups to them that can then attach to antibodies, as described above and in Figure 1. This biocompatible coating is essential to protect the body from direct contact with these iron cores since these MNPs are prone to opsonisation without any coating in vivo. Opsonisation is the process by which phagocytosis takes place to destroy the particle [4], [7]. The superparamagnetic feature is important in MRI detection. Iron oxide nanoparticles

exhibit superparamagnetism, an essential feature because it allows their detection using MRI. For the effects of superparamagnetism to be discernable, every individual nanoparticle core must be small such that it does not have a measurable permanent dipole moment when an external magnetic field is not present, according to *Yigit et. al*. However, superparamagnetism is affected by the surface biomolecules around the cores [7].

Use of Nanotechnology in Cancer Diagnosis Through Polymer Encapsulation:

According to *Yigit et. al* in the review paper, MNPs provide a useful way of detection of cancer because of a use of a noninvasive method with high sensitivity and prevents the use of biopsies, which includes a painful procedure that the patient has to undergo. Moreover, more molecules could attach around the polymer of the nanoparticle to detect the actual cancer cells. More cancer markers are being discovered and more is being known about the different ways cancer cells are expanding and how they are invading the tissues and cells.

A multilayer concept is used for these particles to detect and cure, as described by *Gobbo et. al* in his review paper. This concept includes a therapeutic coating with targeting ligands in addition to the iron core and biocompatible coating, which was described above and shown in Figure 1. This multilayer concept is shown in Figure 3 below.

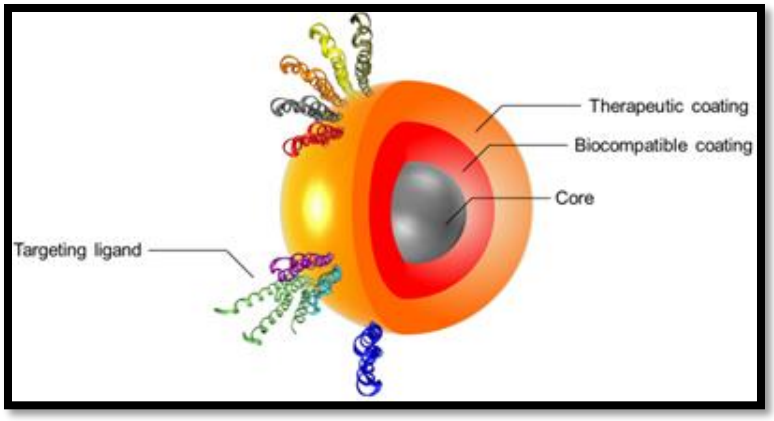

Figure 3: Multilayer concept for magnetic nanoparticle [4]

This therapeutic coating could be another layer or it could be included within the biocompatible coating. These nanoparticles have many therapeutic uses. For example, with magnetic nanoparticles (MNPs), cancer cells can be killed if heat is permeated around them through a high frequency magnetic field [4]. Moreover, *Yigit et. al* states that imaging and therapy can be combined such that biomolecules, such as small interfering RNA (siRNA) or a drug molecule, such as doxorubicin or Gemcitabine, are inserted into the polymer coating of the nanoparticles through covalent or noncovalent bonding or hydrophobic or electrostatic interactions [4],[7]. Doxorubicin is used treat mostly breast, blood, and bladder cancer, whereas Gemcitabine is used to treat pancreatic and bladder cancer. Depending on the conditions of the cancerous cells, pH, temperature, or certain enzymes can help release these drugs from the polymer coating. [4]. Nanoparticles are mostly ejected into the body through intravenous injection, which allows the particles to spread throughout the body into multiple tissues with multiple cancer target cells. RNA interference (RNAi) is important and relies on the fact that the genome sequence of the target must be known. A double stranded RNA is then inserted and blocks the gene of target and prevents from expressing that gene

and producing any proteins. In MNPs, the polymer coating could have molecules around it in order to target the cancer cells. Chemotherapy is limited in its use because it does not target specific types of cancer cells and is also a source of toxicity in the body. Another way to inhibit cancer cells for therapy is to insert drugs into the polymer coating [7]. One such study was done by *Lim et al.,* in which the iron oxide particles were coated with PEG, which consisted of doxorubicin drug with π-π interactions between the pyrene groups of both molecules. Via the process of protonation of doxorubicin in the acidic environments of cancer conditions, the interaction was interrupted and the drug was released from the polymer coating. These nanoparticles were also conjugated with antibodies in order to have a specific target of cancer cells [12]. Drug delivery with nanomaterials is essential because with lower doses, these drugs can react within the body more efficiently, unlike the current pharmaceutical products. However, drug delivery requires that the magnetic particles be targeted on the surface of the body since externally magnetic fields are not strong enough to impact cells in the interior sections and structures of the body [11]. Nanomaterials could also lead to a more direct way of targeting cancerous cells with optimized selectivity due to the targeting ligands and coatings around the iron cores [4].

Thermal therapy includes a heat-based and a cold-based solution. Cryosurgery, a cold-based solution, could be used as a treatment, as described before. Hyperthermic solutions include using lasers, ultrasound waves with high intensities, and an alternating magnetic field. The optical, electrical, and magnetic properties of MNPs are used to destroy cancer cells. An alternating external magnetic field allows heat to be generated to kill cancer cells, as mentioned above. Before heating begins, the nanoparticle is injected directly into blood so that it is able to find the target cells [4].

Most of the therapies do not provide a specificity and converting to a clinical application *in vivo* can be difficult since the knowledge is limited in that area. However, these cells can be detected noninvasively. MRI, single photon emission computed tomography (SPECT), and positron emission tomography (PET). SPECT and PET have a higher sensitivity than MRI, but poorer spatial resolution. MRI provides a better way for soft tissue characterization. MNPs can be used as T2 contrast agents and can be used for drug delivery in the body as therapeutic agents for cancer [7]. Nanoimaging provides a way to detect and diagnose cancer earlier with this MNPs and the MRI system.

Targeting Cancer Cells with MNPs:

There are two ways of targeting cancer cells: passive and active targeting. Tumors develop and create their own blood supply and vessels, which are leaky due to their abnormality. Through passive targeting, these MNPs can enter these leaky vessels and can go to the cancerous cells. Passive targeting depends on the properties of the MNPs, such as size, surface charge, and hydrophobicity. For sizing, smaller MNPs (about 20 nm) accumulate mostly in kidneys, whereas medium MNPs (about 30-150 nm) collect in the bone marrow, hearth, kidney, and stomach, according to *Gobbo et. al* [4]. The large MNPs are mostly in the liver and spleen. Smaller MNPs can accumulate more easily in cancerous areas because they can enter and leave more easily due to the enhancement permeability and retention (EPR) effect caused by the abnormal growth of blood vessels by cancer cells. In other words, accumulation of these MNPs occur more in abnormal cells than normal cells. In addition, hydrophobic and positively charged particles last longer than hydrophilic and negatively charged MNPs because of opsonisation. Even though passive targeting seems to target tumors, it is not as efficient and needs a more direct way of targeting.

Active targeting provides a more direct way of contact with the cancer cells by attaching ligands as surface modifications of the MNPs. Another way is to be encapsulated into other structures of the nanoparticles, such as liposomes or micelles. Cancer cells have certain biomarkers that are overexpressed and can be targeted easily by these ligands on the MNP. For example, monoclonal antibodies are used to target endothelial growth factors on cancer cells. Peptide ligands are attracted to overexpressed surface receptors on cancerous cells, which can also help detect them [4]. For example, a protein called nucleolin is overexpressed in tumor cells and a synthetic ligand called N6L could be attached to the nanoparticle to help detect the unhealthy cells and trigger apoptosis, as explained by *Destouches et. al* [13].

Summary of the Advantages of MNPs in Cancer Treatment:

In summary, MNPs have shown to have multiple advantages, as described by *Gobbo et. al*. First, they can be used to target cancer cells directly and can be used as a contrast agent for an MRI system due to their paramagnetism. Second, these MNPs could be beneficial in thermal therapies and heat generation in the tumor cells to destroy them. Third, they are biocompatible and could be used *in vivo* conditions. Moreover, the use of these particles combines detection, diagnosis, and therapy all in one method. Thus, these multifunctional MNPs are ideal for use for targeting and killing cancer cells. Gadolinium has been used as a contrast agent as well, but it has proven to be toxic in the body in addition to affecting environmental conditions negatively. After gadolinium has been used in patients as a contrast agent, it is usually released from the body through urine and waste. This product is ultimately found in rivers and lakes and is also absorbed by plants, which is then consumed in various foods by humans. Therefore, another contrast agent is needed to be used for MRI

signaling. Iron oxide nanoparticles provide doctors and clinicians with many features and functions since they are found in nature and provide a safety for the environment [4].

Study of Using Bioorthogonal Chemistry and Bonding for Cancer Detection:

A case study has shown that biorthogonal chemistry between biomarkers on targeting cells and nanoparticles can prove to be a technique to target tumors with great specificity. Direct and specific targeting is challenging, but this method provides a way to improve the detection process. Targeting has been difficult because of not being able to differentiate between the target and other background molecules. Therefore, there is a need for enhanced nanomaterial-based detection and delivery. This study has shown that biomarkers, such as HER2 and EGFR on cancer cells, have been targeted by modified nanoparticles through a technique called biorthogonal nanoparticle detection (BOND). This method uses an irreversible inverse Diels-Alder reaction between a tetrazine (Tz) and a strained dienophile, such as trans-cyclooctoene (TCO), to attach nanoparticles to biomarkers, as stated by *Haun et. al.* In this method, monoclonal antibodies would be modified with this TCO structure and nanoparticles would be attached to Tz in order to enhance the nanoparticle binding and signaling. This covalent bond between the TCO and Tz would create a nanoparticle that could specifically target cancer cells due to amplified binding. Monoclonal antibodies are used mainly because they have primary functional amine groups, such as lysine residues, available, that can easily attach to various nanoparticles. The more sites that are available, the higher the detection and signal is. Moreover, Tz acts as an ideal molecule because it has a high valency and it is small and can attach to the TCO sites without having a physical limitation on the nearby sites [6],[14]. Figure 4 shows this BOND mechanism in which an antibody has been modified with the TCO structure and a magneto-

fluorescent nanoparticle (MFNP) has been attached to a Tz molecule to attack surface markers, such as cytoplasmic (cytokeratin, CK) and nuclear (Ki-67) biomarkers [6].

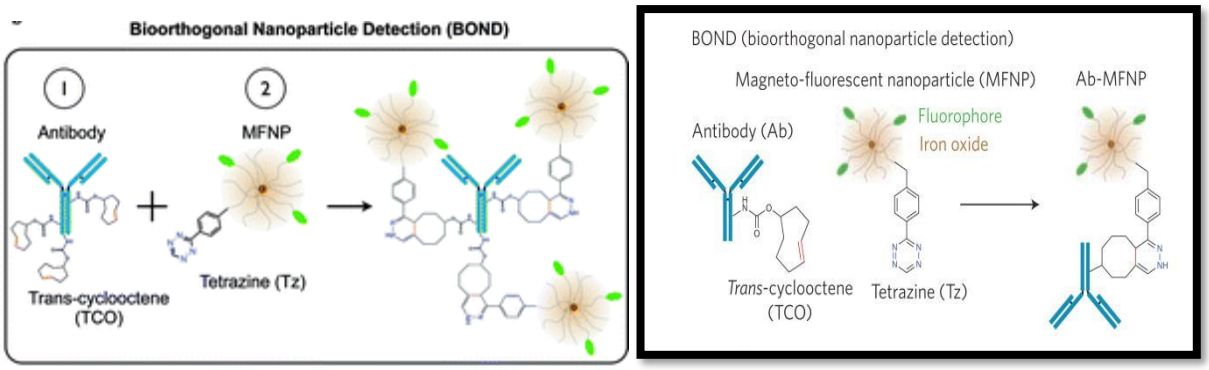

Figure 4: Two images of BOND Between TCO Modified Antibody and Tz Nanoparticle [6],[14]

Diagnostic magnetic resonance (DMR), nuclear magnetic resonance (NMR), and flow cytometry were then used to see the results and sense the nanoparticles and gain visual images of the morphological information. With this method, there can be multiple nanoparticles attached to each antibody and thus, increasing signals when attached to surface markers. In contrast, direct binding of nanoparticles to antibodies limits it to one nanoparticle per antibody. This method of attaching one antibody to on nanoparticle is called BOND 1, whereas the method described with the TCO modified antibody covalently bonded to a Tz nanoparticle is called BOND 2, as shown in Figure 5. This study has shown that BOND 2 works more efficiently than the other method.

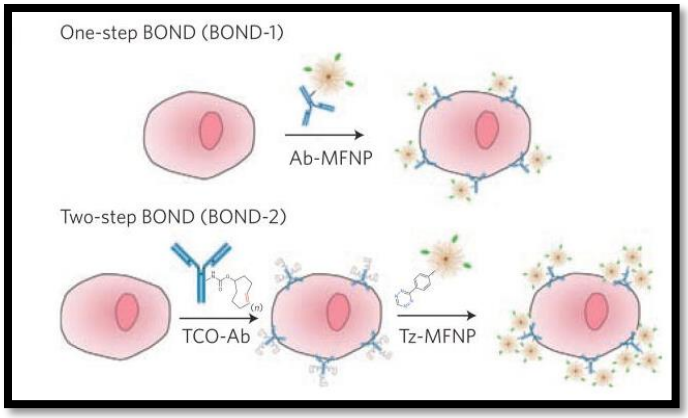

Figure 5: Difference Between BOND 1 and BOND 2 [14]

This BOND method is adaptable to metal nanoparticles and can be used in magnetic nanoparticles to amplify binding, increase sensitivity, and increase specificity of molecular profiling and targeting of cancer cells, unlike the other immune-conjugation methods used, as stated before [6], [14].

A flow diagram is shown below in Figure 6 to summarize the process of everything described above. Currently, stabilizing the molecule in aqueous environments after a coating layer is essential and needs more focus. This thesis describes the process for working on creating a stable molecule and mostly, preventing aggregation and micelles from forming. After the MNPs are stabilized, cancer detection is possible through attachment of functional groups and antibodies to target cancer cells and through MRI signals. After that process is working, therapeutics with heat therapy and drug delivery are possible.

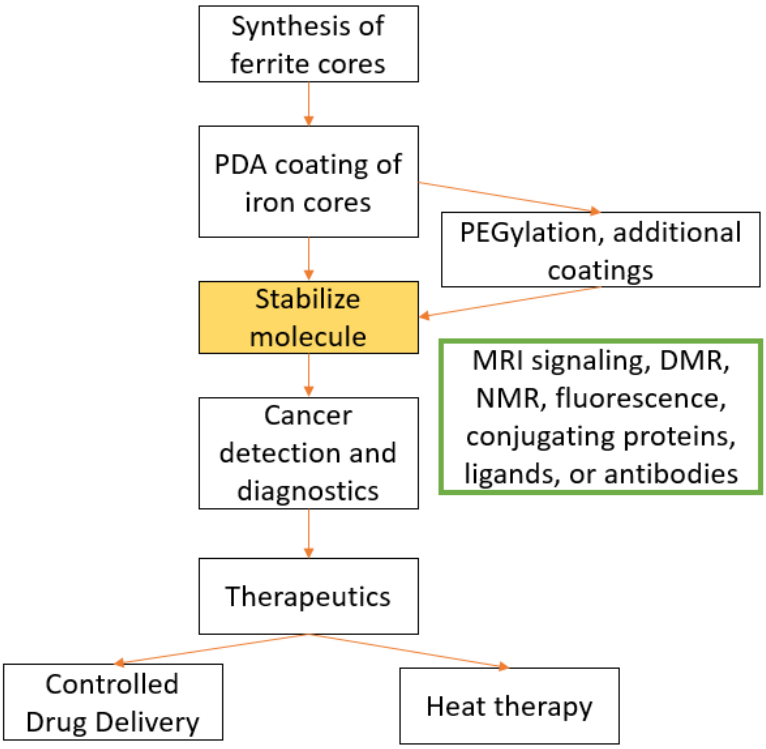

Figure 6: Flow diagram of Process to Therapeutics

CHAPTER 2: METHOD HISTORY AND EXPERIMENTS DONE IN THE PAST

Initial Concept of Self-Assembly of Phospholipid – PEG Coating through Dual Solvent Exchange:

Tong et. al describes a method of a phospholipid PEG coating around iron oxide cores for biomedical applications of nanoparticles in order to provide a water-dispersible particle in vivo and in vitro, prevent aggregation, and reduce adsorption with other molecules. Moreover, the density and amine reactive groups on nanoparticles are important for bioconjugation and allows them to provide a way to target cancer cells more efficiently. Hydrophilic molecules are coated around these nanoparticles since aggregation is possible in aqueous solutions. Covalent bonds are formed between hydrophilic molecules, with sulfhydryl and carboxyl groups, and nanoparticles. However, challenges arise because of coating hydrophilic polymers onto hydrophobic molecules. Amphiphilic polymers can solve these issues and interact with the hydrophobic surface of the nanocrystals. PEG provides a low critical micelle concentration (cmc) and provides a way for adsorption to occur between the hydrophobic nanoparticle and polymer with the hydrophilic regions of the polymer exposed to the environmental and aqueous conditions [8].

In this study, two methods to make water-dispersible nanoparticles with their coating are a film hydration method and the solvent exchange method. In the film hydration process, the nanoparticles with hydrophobic surfactants and amphiphilic polymer are dispersed in chloroform and then chloroform is evaporated with a rotary evaporator, which results in a thin film and form water-dispersible nanoparticles in aqueous solutions. Energy from heat and sonication is needed for this process. However, issues that can occur with this method are the formation of empty micelles from the polymer and aggregation. High surface energies of the nanocrystals result in aggregation, which is not reversible in these conditions. To avoid

aggregation, there needs to be an intermediate component between the coating and nanocrystals during the thin film process to separate the nanocrystals. Nonsolvents can help in changing the surface properties of nanoparticles to stabilize the reaction between the nanoparticle and coating. A solvent exchange method is described in this study to maintain the monodispersity of these nanoparticles. In this method, a sudden change or transition occurs from a solid thin film to forming a colloidal solution. This is done immediately after chloroform dispersion occurs and chloroform is slowly substituted by dimethyl sulfoxide (DMSO). After that, chloroform is evaporated using a vacuum because chloroform has a low boiling point and then DMSO is replaced by water by washing using centrifugal filters to ensure the binding of the polymer to the nanocrystal. In summary, this procedure allows for a slow transition from chloroform to water with ascending polarity. DMSO helps in the assembly process of the nanoparticles while water helps to solidify the structure. The film hydration and dual solvent exchange method are shown in Figure 7. Orange is the chloroform, green is DMSO, and blue is water [8].

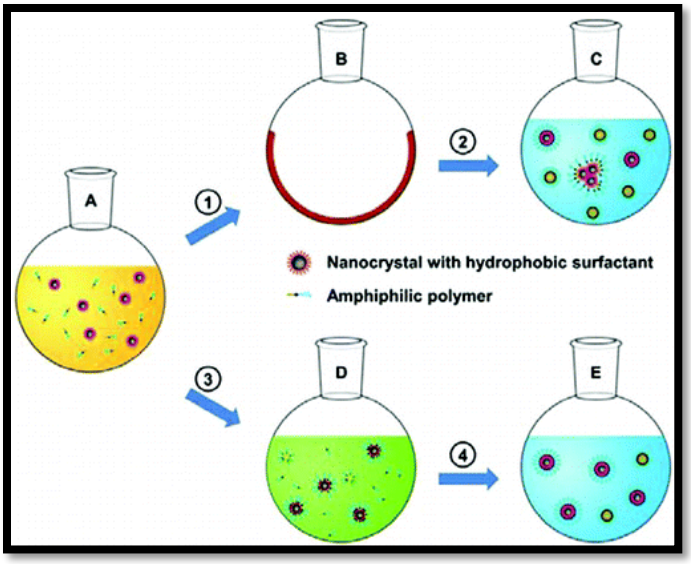

Figure 7: Film Hydration Method vs. Solvent Exchange Method [8]

Use of Polydiacetylenes for Iron Oxide Cores:

PEG has been shown to be a useful polymer to act as a coating for iron oxide nanocrystals. However, studies have shown, according to *Hoffman et. al,* that because of the large sizes and lengths of these polymers, they significantly increase the diameter of the nanoparticle, which might not work for MRI systems since they require small molecules for detection [15]. However, they can still be used to protect and stabilize the particles in an aqueous environment.

Polydiacetylenes, or PDAs, are chromatic polymers that have been shown to have efficient chemo- and bio- sensing, according to *Jelinek* [16]. PDAs have been an attractive option because of their chromatic properties and their ability to be able to change colors in the visible spectrum, which can be noticed with the naked eye. PDAs can be polymerized through ultraviolet, or UV, irradiation and absorb light in the visible spectral region, thus emitting blue color in this process. Fluorescence properties have also been an attractive feature since PDAs can exhibit strong fluorescence when changing from a blue phase (640

nm) to a red phase (500 nm). This colorimetric feature of PDA is shown in Figure 8. The crosslinking that happens due to UV treatment allows PDA to become blue, whereas a change in C-C bond structures can convert the phase into a red color. However, scientists are still not completely clear on the chemical properties of the transition from blue to red [16]. The first image on the left shows a diacetylene in an unclear state and due to polymerization and crosslinking of the bonds, changes to a blue color. The image on the right and on the bottom show the changes that occur chemically and physically due to polymerization and then heating when changing from a blue to red color [16], [17], [18].

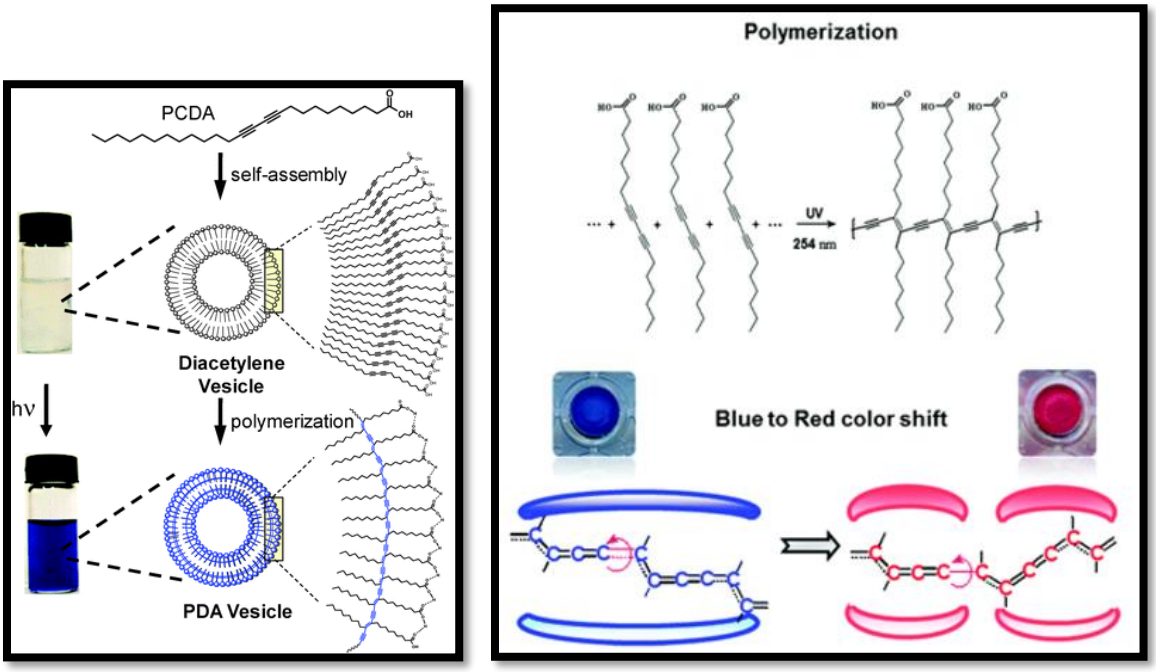

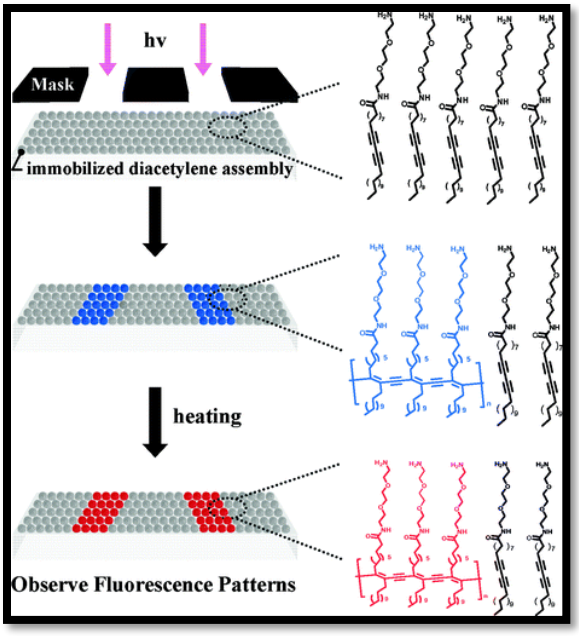

Figure 8: Colorimetric Properties of PDA [16], [17], [18]

PDA is formed from a bunch of diacetylene monomers that are attached via 1,4 addition, which occurs due to polymerization by using a UV light with a 254-nm wavelength. Diacetylene monomers alone cannot absorb visible light, however, polydiacetylene polymers are able to do that and appear blue because of an electron delocalization in the linear π bond, which creates a π-π* bond transition and thus, creates an alternating ene-yne polymer chain. Moreover, PDAs do not consist of any impurities because the polymerization process does not include any catalyst or enzyme to start the reaction process [16], [17]. Figure 9 below shows the PDA coating around magnetic cores and polymerization creating a blue color and in addition, a red color transition from blue when an external magnetic field is applied, which is able to generate heat on the nanoparticle surface. This is known as a magnetochromic effect, which utilizes the optical and electrical properties of PDA. The color at room temperature is blue and it slowly transitions to a purple and red color as it is heated to approximately 90 degrees Celsius [16], [18].

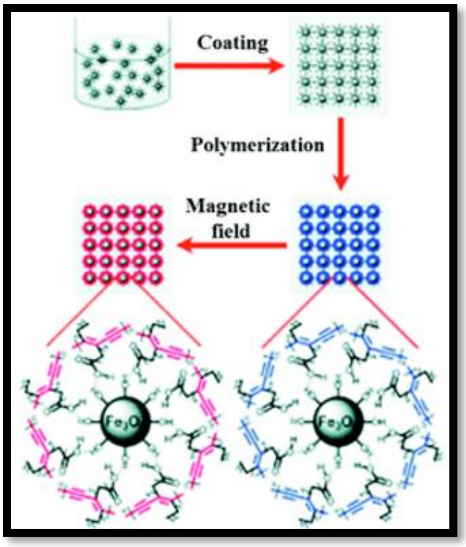

Figure 9: PDA coating around Iron Oxide Cores [16]

One such PDA molecule is 10,12 pentacosadiynoic acid (PCDA), which has proven to be nontoxic and more stable since they are polymerizable, unlike other molecules that cannot be polymerized. According to *Fang et. al,* studies have shown that since PCDA has optical and chromatic properties that are highly beneficial due to their sensitivity to pH and temperature changes and PCDA molecules could be used for SPION [19],[20]. Another PDA molecule is 10,12 heptacosadiynoic acid (HCDA), which has the same properties of all PDA molecules. The structures of the PCDA and HCDA molecule are shown below in Figure 10. The first picture on the top shows the chemical formula of PCDA (12a), whereas the second picture below it shows the crosslinking between PCDA after polymerization (12b), and the third picture below that one shows the chemical formula of HCDA.

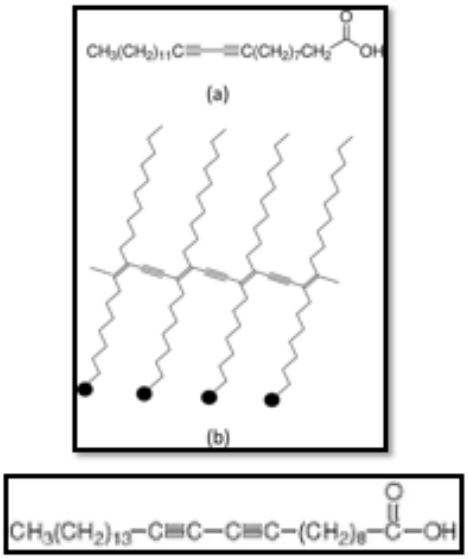

Figure 10: PCDA Chemical Formula and Structure, HCDA Chemical Formula [20], [21]

As shown, these structures have a carboxyl group attached. When they are coated around iron oxide cores, the carboxyl groups stick out and are used to bind to other components, such as PEG or another biocompatible molecule or an antibody, as can be seen in Figure 11 [17].

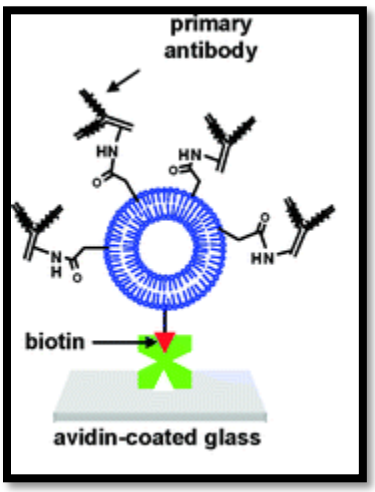

Figure 11: PDA Structure with Primary Antibody [17]

Process of PEGylation after PDA coating:

The process of amine PEGylation is used to modify nanoparticles to make them more soluble and stable in aqueous solutions. The (PEG)n-amine could be used and is coupled to a surface with carboxyl groups by using EDC (1-Ethyl-3-(3-dimethlaminopropyl)carbodiimide HCl) and NHS (N-hydroxisuccinimide) or sulfo NHS as coupling reagents. PEG amine reagents can form hydrophilic groups with methyl ether terminations with some exposed carboxy termination groups, which are then attached to affinity ligands using the coupling reagents in a carbodiimide coupling reaction [22]. This reaction is used to couple carboxylic acids of liposomes with primary amine groups of the PEG via amide bonds. Carbodiimide compounds, such as water-soluble EDC and NHS or sulfo NHS, are used for crosslinking to carboxylic acids. The advantage of these compounds is that they disappear in the final product and only the desired conjugated products are present. Figure 12 shows the process in which an EDC molecule is attached to a carboxylic acid terminated group, which creates an intermediate that is not stable in aqueous solutions. Therefore, sulfo NHS is added to create a dry stable, or amine reactive, and is coupled to the carboxyl groups by EDC.

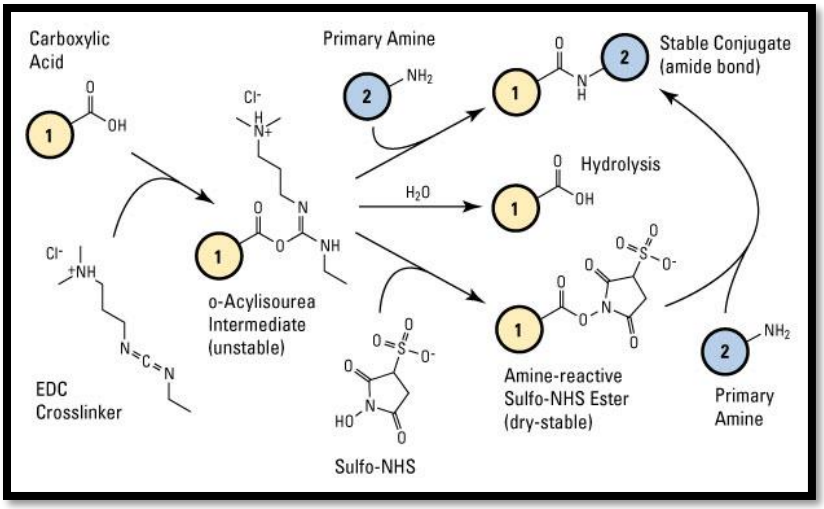

Figure 12: Carbomiide Reaction Using Coupling Reagents [23]

Ultimately, a product is formed with reactive amine groups on one end and methoxy groups (nonreactive) on another end [23]. In addition, these amine groups can react with other biocompatible and desirable molecules and PEGs for specific targeting.

Quantification of Iron Oxide Nanocrystals:

When iron oxide nanoparticles are coated, it is also necessary to determine quantitatively how much iron is present. A compound called ferrozine, for which the structure is shown in Figure 13, is known to act as a bidentate ligand with metal ions, such as iron.

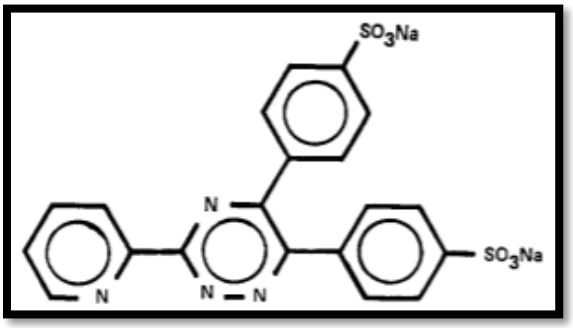

Figure 13: Structure of Ferrozine [24]

This compound, which was found in the disodium salt of 3-(2-pyridyl)-5,6-bis(4-phenylsulfonic acid)-1,2,4-triazine, attaches to iron and is useful for quantitively examining iron. When attached to iron, a magenta color is formed and the molecule is very soluble in water. Absorption could be measured at ferrozine's maximum absorbance, which is 562 nm, and Beer-Lambert Law can help determine the concentration of Fe [24].

Measurements Using DLS and Nanodrop:

Various measurements are needed for characterizing the synthesized and coated nanoparticles. Dynamic light scattering (DLS) and Nanodrop could be used to measure the sizes and zeta potential and the absorbance of the particles. To determine particle sizes in suspension, DLS could be used. DLS provides a mean sizes and distributions of number, volume, and intensity of the particles [11]. Particle sizes are measured using Brownian motion, which is the random motion of particles in a liquid, and their diffusion speed is used to achieve sizes of the particles. [25], [26].

Another feature of measurement for these particles is the surface charge, measured by Zeta potential to determine colloidal stability. This theory forms from the fact that ions in a liquid are attracted to the opposite charges on a nanoparticle surface [27]. A high zeta potential in millivolts, either positive or negative, has a higher stability since the electrostatic interaction is higher between positive and negative molecules between the liquid suspension and nanoparticles, and thus, aggregation cannot occur. However, if the zeta potential is low, then repulsion forces are weaker than the attractive forces within the nanoparticles and thus, aggregation occurs. The voltage range for stability is around +30 mV or -30 mV. Zeta potential is affected by pH [11], [27].

On the other hand, the nanodrop helps in achieving absorbances of the particles. The nanodrop is a UV-VIS spectrophotometer that is used to quantify the purity of proteins and other molecules using optical properties. 1-2 μL of the sample is placed between a source and receiving fiber. Light is speculated using a linear CCD array in a spectrophotometer when a xenon lamp passes light through the sample. Absorbance of the samples can then be read using a PC computer [28].

Past Work from a Previous Student

A master's student from last year in Professor Jered Haun's lab worked on stabilizing these molecules in aqueous environments and trying to extract the small MNPs from the larger particles and liposomes. The student used the dual solvent exchange method to create this coating around the magnetite nanocrystal. This method initially used synthesized cores in hexane that needed to be washed with ethanol in order to remove the hexane and after, toluene was then added for using the cores in the dual solvent exchange method. This mixture was then added to a solution of chloroform and PDA polymer and DMSO was slowly added after that. The chloroform and toluene needed to be removed using a vacuum because these were unwanted solvents. However, this process took a while and was not efficient enough since the vacuum that was used to evaporate these organic solvents, was not stable and resulted in multiple issues. The student had to perform multiple experiments to figure out how to maintain a constant pressure such that all the solvents evaporate from the solution in order to have MNPs that haven't aggregated in the final solution. This task was tedious and did not always lead to desired results of having the correct sizes or non-aggregated solutions. Even though the student was able to figure out a constant pressure value and a method to stabilize the solution, this method did not work with repeatability

efficiently and led to inconsistent results at various points of time. The vacuum was an unreliable source to take out the solvents from the solution. Therefore, a solution was needed in order to possibly remove the need for a vacuum to have more reliable results and stable compounds.

CHAPTER 3: METHOD

Project Overview:

The purpose of this project was to create stable magnetic nanoparticles in aqueous solutions to be able to functionalize them and be used for molecular medicine. Iron cores, which are immersed in toluene and purchased from Sigma Aldrich, are used to provide a PDA coating around them in order to become biocompatible molecules in aqueous solutions. A modified dual solvent exchange method was used, in which the vacuum was removed completely. This method, which eliminated some of the solvents and thus, the need of a vacuum, was used to attach PDA molecules to iron cores, in which particles were first stabilized in DMSO and then DMSO was slowly replaced by water to make more soluble and stable compounds without the use of any chloroform and additional toluene in the solution. The solution was then UV treated the next day for polymerization to occur and then was purified with centrifugal filters to concentrate the samples by removal of extra water and DMSO in the solution. The same day, a ferrozine assay was performed to quantify the amount of iron in the solution. To avoid aggregation, the particles needed to be utilized immediately. After the PDA coating was placed, PEGylation was performed the day after. The process of PEGylation included attaching a PEG amine to a carboxyl group of the PDA coated iron cores. These nanoparticles were tested throughout the experiments for stability using zeta potential and sizes were measured using DLS to obtain number, volume, and intensity results.

Coating Method, Ferrozine Assay, and PEGylation Process:

The previous student used the dual solvent exchange method as is, as described in the section above. 800 µl of chloroform was first added to a flask with the desired amount of PDA. In the meantime, 20 µl of synthesized iron cores immersed in hexane were separated by ethanol via centrifugation. A pellet formed at the bottom of the Eppendorf tube, which consisted of the cores. At least 200 µl of toluene was added to the tube and vortexed. The cores were then added to the flask with chloroform and PDA amount to make a total of 1 mL. 4 mL of DMSO was then added and the solution was put under vacuum to evaporate the solvents. After three hours under the vacuum, the solution resulted in around 2-3 mL when removed from the vacuum. DMSO was then added until 4 mL of solution remained. After thirty minutes of waiting time, 16 mL of water was then added to make the 20% DMSO solution. The process remains the same as the modified dual solvent exchange method after the addition of water, as will be described below.

The current process includes the iron oxide cores, which were first coated with HCDA or PCDA, using the modified dual solvent exchange method, and then a PEGylation process around the PDA coating. A desired amount of PDA molecules was used with purchased 10 nm and 20 nm cores stored in toluene from Sigma Aldrich. Unlike the dual solvent exchange method described above, the vacuum, which was used to evaporate and remove solvents, was eliminated since chloroform was not added and only a small amount of toluene, which was part of the purchased cores, was used in the solution. DMSO was directly added to a solution with a PDA molecule and iron oxide cores. After thirty minutes of shaking and mixing, water was slowly added to the solution to replace DMSO, which resulted in a 20% DMSO solution. After filtering and washing, the volume of the solution was recorded and the same amount of water was added as the recorded volume, thus presenting a 10% DMSO

solution. This solution was then UV treated the next day for polymerization of the PDA molecules to occur to be more stable and to visually be able to see the blue color of the molecules. After UV treatment, the samples were concentrated using the centrifugal filters. Through concentration, excess DMSO and water to help concentrating and purifying the samples. DLS and absorbance readings from the Nanodrop were taken and recorded. The procedure is described below in details.

PDA Coating of Iron Oxide Cores Using Dual Solvent Exchange Method:

Objective: To coat iron oxide nanocrystals with a PDA coating.

Day 0: Coating process:

1. Weight out 3, 5, 10, or 20 mg of the desired PDA polymer – either PCDA (10,12 Pentacosadiynoic acid, 98%) or HCDA (10,12 Heptacosadiynoic acid, 98%) – in round flasks.
2. Add 4 mL of dimethyl sulfoxide (DMSO) to the round flasks with the polymer using a 1 mL pipette. Add DMSO drop by drop.
3. Add 20 microliters of the iron oxide cores (purchased 10 nm or 20 nm cores) into the flasks with the DMSO and PDA molecule.
4. Incubate in the orbital shaker at 85 rpm for 30 mins at 22 degrees Celsius set point.
5. Measure the volume in each flask with the 10 mL polystyrene long pipettes.
6. Add 16 mL of water to each flask to make sure it is 20 mL total volume. Swirl after every 3 mL addition of water. This results in a 20% DMSO solution.
    a. Make sure there are no aggregates at the bottom. (no pinkness)
7. Add 15 mL of each solution to the pink Amicon centrifugal filter tubes 100 K 24 pk.

8. Centrifuge at 3000 rpm for 10 mins in the big centrifuge machine.
9. Use a 1 mL pipette and transfer 5 mL of each solution from the top of the filter to the blue Falcon 50 mL Polypropylene conical tube using the 1 ml cotton syringe filter (made by putting a small cotton ball in a 1 ml syringe).
10. Take the rest of the solutions in the round flasks and transfer it to the pink centrifuge tubes. Centrifuge for another 10 mins at 3000 rpm.
11. After time, throw the excess liquid that passed through the filter in the waste.
12. Put the rest of the solution into the blue tubes using the cotton syringe filters.
    a. Make sure to record the volume. For the last bit of transfer, make sure to calculate how much is in the green syringe before squirting it all out into the blue tubes. Make sure to subtract 0.1 mL that accounts for the cotton.
13. For ferrozine assay, take out 50 microliters of the 20% DMSO solution of each in an Eppendorf tube.
14. Add 50 microliters of 36.5-38% HCL into the Eppendorf tube.
15. Vortex the tube.
16. Add water with the long plastic pipettes to the blue tube with the same volume that was calculated before after using the cotton syringe filters.
    a. Add 3 mL of water dropwise at a time and mix in between.
    b. This becomes a 10% DMSO solution.
17. Store the blue tube solutions in the -4 C fridge and store the Eppendorf tubes for ferrozine assay at room temperature.

Day 1: UV treatment, DLS, and Nanodrop:

1. Make sure the UV light is at short wavelength. Use the 12-well plate and transfer 6 mL at a time to 2 of the wells and UV treat for 20 mins. Keep repeating until all solutions are UV treated.
2. Transfer all the UV treated solutions into a new set of blue tubes.
3. Save 1 mL of each UV treated solution in an Eppendorf tube for DLS and absorbance results.
4. In the meantime, do the ferrozine assay of the 50 microliter samples from Day 0.
5. Take nanodrop values of all of them – 3 times for the original, 1 time for the control, and 1 time for the UV treated.
    a. Nanodrop wavelengths: 640 nm for the UV treated. 562 and 810 nm for the control and original.
    b. Use the 20% DMSO blank for the control and original and use the 10% DMSO blank for the UV treated.
6. Take DLS of the unconcentrated UV treated solutions on Day 1.
7. After taking DLS of the 1 mL solutions, concentrate the samples. Transfer 15 mL of the unconcentrated, UV treated solutions into Amicon centrifugal filter tubes 100 K 24 pk.
8. Centrifuge in the big centrifuge for 5 mins at 3000 rpm or 3 mins at 2000 rpm.
9. Throw the excess liquid into the waste and then transfer the rest of the solutions from the blue tubes into the pink filter tubes. Keep the right balance in the centrifuge. Centrifuge again.
10. Add the 1 mL UV treated solution from the Eppendorf tubes into the pink filter tubes and mix it inside with the aggregates.

11. Take the concentrated solution from the top filter after mixing and put it back into the Eppendorf tube using a syringe cotton filter, made similarly to the previous one.
12. Take the nanodrop and use 10% DMSO as the blank.
13. Take DLS and absorbance readings for concentrated solutions as well.

A ferrozine assay was then used to quantify the amount of iron oxide particles in a sample. This was done by taking 20% DMSO solution and adding hydrochloric acid to it in order to break the PDA coating around the iron oxide cores. Bases were then added in to neutralize the acidic chemicals. After that, the solution was divided into two tubes – one to act as a control with just water and one with added ferrozine in order to measure the amount of iron content. Thus, the ferrozine would attach to the iron content and be able to measure the absorbance value at 562 nm and 810 nm. The ferrozine assay protocol is described below in details.

Ferrozine Assay:

Objective: To quantify the amount of iron oxide in sample.

1. Overnight incubation of 50 µL sample from Day 0 of 20% DMSO solution with equal volume of 12 M HCl was necessary.
2. Add 240 µL of 2 M NaOH, 50 uL of 4 M ammonium acetate, and 110 uL of 5% hydroxylamine HCl sequentially into solution.
3. Incubate at room temperature for 30 min.
4. Mix 250 µL of solution with 250 µL of 0.02% ferrozine solution.
5. Mix 250 µL of solution with 250 µL of diH_2O to make a control.

6. Measure absorption of ferrozine and control. Light absorption was read at 562 nm with 810 nm as reference.

Pegylation was then done on top of these coatings using the carbodiimide reaction process to be able to attach the carboxyl groups of the liposomes and amine PEGs using coupling agents, EDC and NHS. A particular concentration of PEG was needed for this protocol and in this case, it was 0.2mmol/L of PEG. In addition, a volume of 1.5 ml was desired by the end of the reaction. Thus, using the desired PEG concentration and the desired volume, a molar equivalence was calculated for all components. Using the molecular weight, the amount of EDC, NHS, and PEG was calculated. The concentration of each of these solutions in water was arbitrary, which was 10mg/ml solution.

PEGylation Process of Coated Iron Oxide Nanoparticles:

Day 2: PEGylation

Objective: PEGylate PCDA-coated magnetic particles with mPEG via EDC coupling between carboxy-terminated particles and amine-functional mPEG..

Pre-requirements: Need 1 ml of liposome solution. This procedure applies to adding a 0.2 mmol/L $mPEG_{112}$-NH_2 concentration of mPEG into a liposome solution to have a desired total volume of 1.5 ml.

1. Weight out each molecule:
    a. NHS (N-Hydrosucinimide) – room temperature – 0.034527 mg.
    b. EDC (N-3-Dimethylaminopropyl N’ ethyl carbidiimide hydrochloride) – (-20 C fridge) – 0.05751 mg.

c. $mPEG_{112}$-NH_2 – Amino PEG, mPEG-NH2, MW 5000 (Methoxyl PEG Amine) – (-20 C fridge) – 1.5 mg.

2. Add the Nanopure water to make it a 10mg/ml concentration solution.
    a. NHS – 3.4527 microliters
    b. EDC – 5.751 microliters
    c. $mPEG_{112}$-NH_2 – 150 microliters
3. Add this much solution to the designated liposome solutions.

Material:	0.2 mmol/L $mPEG_{112}$-NH_2
Liposome (mL)	1
EDC (microliters)	5.75
NHS (microliters)	3.45
mPEG (microliters)	150
H20 (microliters)	340.80

4. Cover with foil and incubate at room temperature for 3 hours.
5. After incubation, purify the samples using the Amicon Centrifugal filters – 4 mL, 10k filters. Add all the solutions from the Eppendorf tubes to the filters. Add water until 4 mL is occupied in the filter.
6. Centrifuge at 3500 rpm for 10 mins in large centrifuge.
7. Remove the liquid that passes through the filter.
8. Add more water until it reaches 4 mL.
9. Centrifuge at 3500 rpm for 10 mins in large centrifuge.
10. Add more water until it reaches 4 mL.
11. Centrifuge at 3500 rpm for 10 mins in large centrifuge.
12. Concentrate down to 1.5 ml. Add water until desired volume is reached.
13. Take DLS measurements of samples the next day and a few hours after PEGylation process.

This is a precise process to coat PCDA or HCDA on purchased 10 nm and 20 nm cores. Results and discussion in the next chapter will describe what measurements were taken and the conclusion of which PDA molecule was better.

CHAPTER 4: RESULTS AND DISCUSSION

An important characterization of these nanoparticles was their size measurements for both HCDA and PCDA polymer coatings for both purchased 10 and 20 nm cores. After UV treatment of the samples the next day, sizes of the nanoparticles with DLS were taken to describe the sizes of the smallest to largest particles in suspension. There are three categories that sizes are divided into: small, medium, and large sizes. These small sizes mostly refer to coated MNPs (20-30 nm), medium sizes refer to larger MNPs (50-100 nm), and large sizes refer mostly to liposomes or micelle populations (200 nm+). Sizes were taken for two conditions: unconcentrated samples after UV treatment and concentrated samples after using the centrifugal filters and green syringe filters. The three best experiments for size characterization were used for each HCDA amount (3, 5, and 10 mg HCDA) and put in the figure below, Figure 14. Three runs of DLS were performed and taken for each sample for number, volume, and intensity. Out of that data, the three best data points were extracted from the best experiments, according to number, volume, and intensity, and were collected for sizing and placed in the chart below. Standard error bars can also be shown in the chart. The data labels include the average sizes of the particles. As can be seen from the chart, the average sizes of the nanoparticles for purchased 10 nm cores for unconcentrated and concentrated samples were approximately in the range of 23.74 to 35.56 nm, 89.34 nm to 106.50 nm, and 187.50 to 206.50 for small, medium, and large sized particles, respectively, for the different amounts of HCDA.

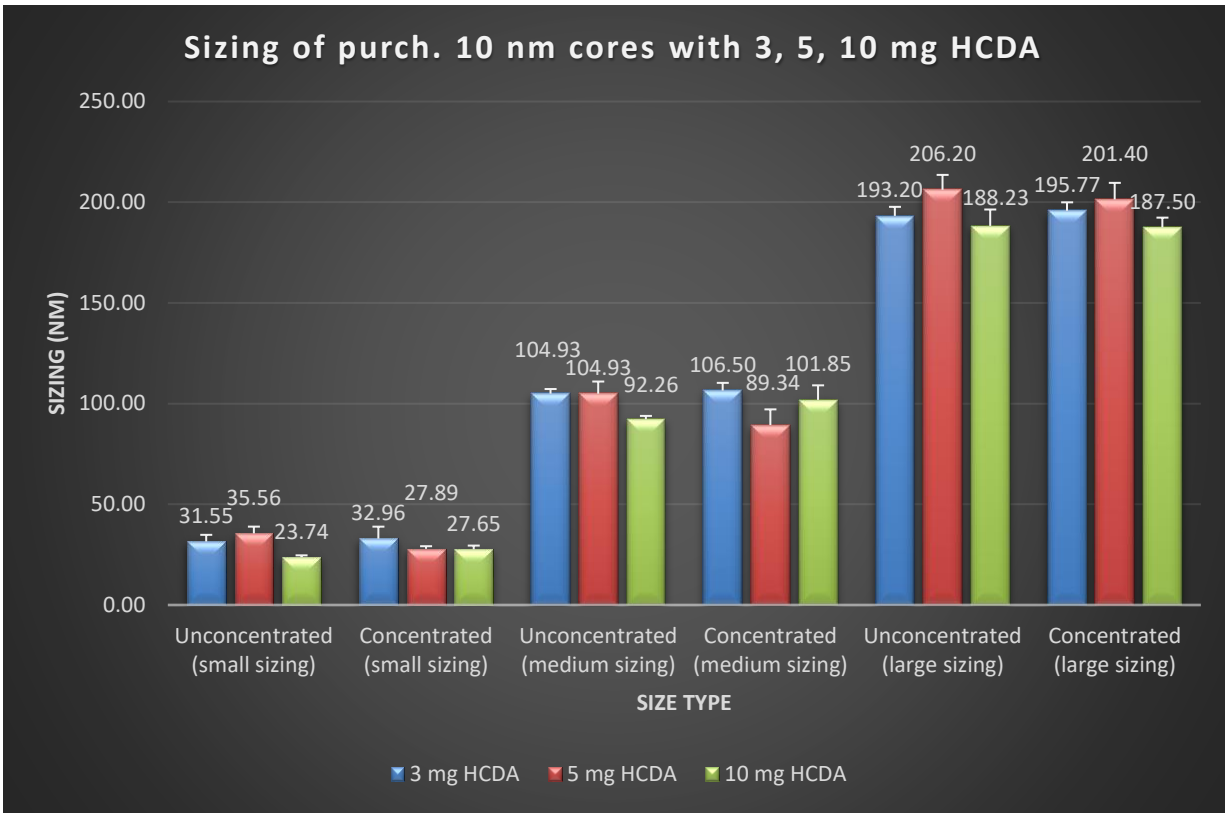

Figure 14: Sizing of Purchased 10 nm cores with HCDA Samples

As can be seen from Figure 15, the average sizes of the nanoparticles for purchased 10 nm cores for unconcentrated and concentrated samples were approximately in the range of 23.66 nm to 31.32 nm, 80.39 nm to 103.84 nm, 185.70 nm to 206.77 nm for small, medium, and large sized particles, respectively, for the different amounts of HCDA. Concentrated sample sizes were similar to the unconcentrated sample sizes. When samples are concentrated, by removing water and DMSO, the samples have more particles in them and thus, concentration of the MNPs increase as well. Samples of desired sizes were more easily extracted when concentrated. In other words, in concentrated samples, less liposomal sizes were present and more of the smaller sizes of the MNPs were present, proving that concentration helps in extracting more of the smaller sizes in the solution.

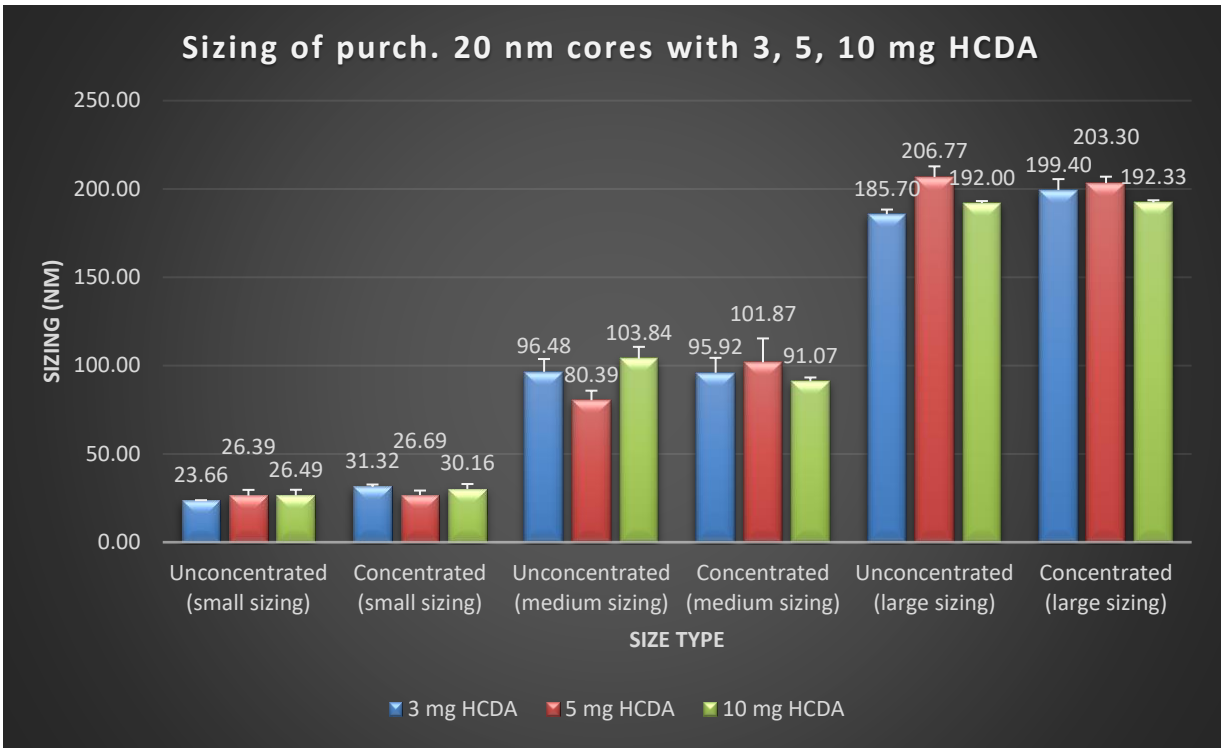

Figure 15: Sizing of Purchased 20 nm cores with HCDA Samples

On the other hand, different amounts of PCDA samples were run with 20 nm purchased cores. These sizes were much larger and more diverse than HCDA samples. Figure 16 below shows these results. The average sizes of the nanoparticles for purchased 10 nm cores for unconcentrated and concentrated samples were approximately in the range of 34.30 nm to 46.51 nm, 49.60 nm to 130.07 nm, 232.87 nm to 246.23 nm for small, medium, and large sized particles, respectively, for the different amounts of PCDA. As shown, these sizes are much more variable, do not have as much consistency in the results, as HCDA samples do, and have more overlapping results between the different size types. Moreover, these sizes are larger than the HCDA samples and thus, could be misleading because of more likeliness of liposome populations to occur. HCDA has a longer alkyl-tail and thus, it could self-assemble on the iron oxide cores to create a stronger bonded layer around the cores.

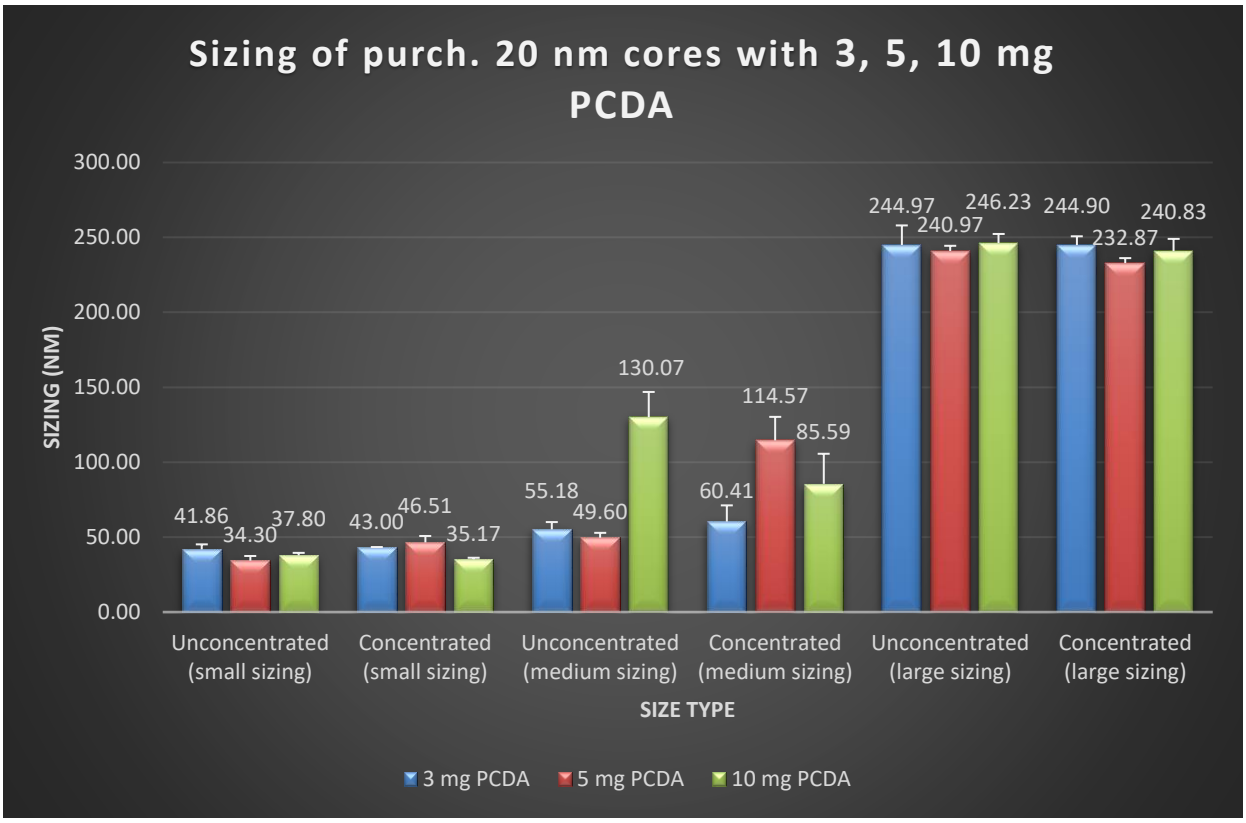

Figure 16: Sizing of Purchased 20 nm cores with PCDA

Results of all the averages, standard deviations, standard errors, absorbances, and percent yields of the three best experiments for 3, 5, and 10 mg HCDA samples with purchased 10 and 20 nm cores and 3, 5, and 10 mg PCDA samples with purchased 20 nm cores are shown in the appendix. Percent yields from the ferrozine assay were calculated based on a standard curve, in which absorbance values were taken as the solution was diluted with different toluene volumes, depending on the type of purchased cores. Absorbances were taken of the ferrozine sample to determine a percent yield by comparing to the standard curve. As can be seen in the data in the appendix, averages for the percent yields for purchased 10 nm cores were 24.43%, 33.63%, and 26.27% for 3, 5 and 10 mg HCDA samples, respectively. Averages for the percent yields for purchased 20 nm cores were 24.93%, 21.37%, and 27.90% for 3, 5, and 10 mg HCDA samples, respectively. Results were

similar for the purchased 10 nm and purchased 20 nm cores. However, results for PCDA were a little lower than the HCDA results. Averages for the percent yields for purchased 20 nm cores were 11.80%, 16.17%, and 21.07% for 3, 5, and 10 mg PCDA samples, respectively. However, when the absorbances were measured before and after concentration and measured at a 640-nm wavelength, the PCDA samples had higher values than HCDA samples. The average absorbances for unconcentrated and concentrated samples for purchased 10 nm cores were 0.097 and 0.274, 0.161 and 0.384, and 0.207 and 0.324 with 3, 5, and 10 mg HCDA samples, respectively. The average absorbances for unconcentrated and concentrated samples for purchased 20 nm cores were 0.068 and 0.181, 0.195 and 0.377, and 0.275 and 0.511 with 3, 5, and 10 mg HCDA samples, respectively. The average absorbances for unconcentrated and concentrated samples for purchased 20 nm cores were 0.147 and 0.372, 0.241 and 0.518, and 0.405 and 0.758 with 3, 5, and 10 mg PCDA samples, respectively. As shown, the sizing results and percent yields of HCDA samples were better than PCDA samples. Moreover, a higher absorbance value is an indication of more liposomes due to a higher polymer concentration. Sizing from DLS and percent yields are a better representation of how stable and biocompatible the particles will be. Therefore, HCDA seems to be a better PDA molecule to be coated around iron oxide cores than PCDA.

These results have been consistent with previous results done by the previous master's student from 2016 in the same project. Her thesis consisted of synthesized cores in the lab, instead of purchased cores from Sigma Aldrich. HCDA sample sizes were an average of 34.5±2.1 nm, 25.5±1.6 nm, 27.8±1.8 nm, and 26.9±1.8 nm for 2, 5, 10, and 20 mg of HCDA, respectively. PCDA sample sizes were a little larger and were an average of 39.6±6.0nm, 40.5±4.9 nm, 46.2±4.2 nm, and 56.8±4.0 nm for 2, 5, 10, and 20 mg HCDA, respectively.

Moreover, the percent yields for HCDA and PCDA ranged from 26-41% and 32-45%. Larger nanoparticle ranges occurred from 200-300 nm that could also result from aggregation or liposome populations. Overall, the HCDA samples in the previous project had sizes of 25-35 nm and PCDA samples had sizes of 40-60 nm, which is similar to the results with the purchased cores shown presented in this thesis project.

PEGylation has also been done on some of the MNPs with the desired sizes of about 20-30 nm. As described above, different amounts of coupling reagents and PEG have been used depending on the PEG-amine concentration that is needed in the sample. The most stable condition has been about 0.2 mmol/L of PEG-amine. Zeta potential was calculated for one of the samples with 5 mg of HCDA around purchased 10 nm cores, before and after PEGylation to see how the surface charge was affected. The zeta potential went from about -41.1 mV to about -25.7 mV. This result is consistent with the chemistry since carboxylic acids protrude from the coating before PEGylation, which has a negative charge, and amine groups are added during PEGylation process to make it a more positive charge and thus, seeing the zeta potential become more positive. In another experiment with samples of 5 mg HCDA around purchased 20 nm cores, sizing was also taken into consideration. After pegylation with 0.2 mmol/L of PEG-amine of the particles, the average size of the particles using DLS was 113.4 nm. This result suggests that there is some aggregation of the MNPs. More experiments need to be performed to get more accurate and correct results for DLS sizes.

CHAPTER 5: CONCLUSION AND FUTURE DIRECTIONS

Functionalized iron oxide nanoparticles have many benefits of acting as a molecular detection and analysis of cancer cells and for therapeutic purposes in the future. There are multiple properties, such as magnetic, chromatic, optical, electrical, and more that can be utilized for molecular medicine. These iron oxide nanoparticles can have more functionalized groups, such as antibodies and proteins, attached that can help detect surface biomarkers of cancer cells. These coatings are necessary to be able to convert the hydrophobic nanocrystals to hydrophilic structures by adding amphiphilic molecular structures to make them more soluble in aqueous solutions. PDA molecules provide a great way for a coating around iron cores because of their ability to change to various colors when UV treated and heated. The dual solvent exchange method provides more stability to these nanoparticles. To test for aggregation and stability, sizes are measured using DLS and zeta potential. The results showed that HCDA coatings were better than PCDA coatings around iron oxide nanocrystals due to their structure, based on DLS sizes, percent yields, and absorbance values.

For now, more stability is needed in aqueous solutions for the MNPs and the aggregation is also an issue that needs to be solved. In the future, once stability has been achieved, more functionalized molecules can be conjugated. Successful development in these areas will help achieve functional nanoparticles for detection in research and industry in molecular medicine to improve quality of life and mortality rates due to cancer [29]. Therefore, more research is being done on these MNPs for cancer diagnosis and therapeutic purposes.

REFERENCES:

[1] Surveillance Epidemiology and End Result Program, “Cancer Statistics - National Cancer Institute,” *Annual Report*. 2016.

[2] "Cancer." Internet: https://medlineplus.gov/cancer.html, [May 31, 2017].

[3] "Cancer." Internet: https://familydoctor.org/condition/cancer/?adfree=true, [May 31, 2017].

[4] O. L. Gobbo, K. Sjaastad, M. W. Radomski, Y. Volkov, and A. Prina-Mello, “Magnetic nanoparticles in cancer theranostics,” *Theranostics*, vol. 5, no. 11, pp. 1249–1263, 2015.

[5] "Haun Lab." Internet: http://haun.eng.uci.edu/, [May 31, 2017].

[6] J. B. Haun, N. K. Devaraj, B. S. Marinelli, H. Lee, and R. Weissleder, “Probing intracellular biomarkers and mediators of cell activation using nanosensors and bioorthogonal chemistry,” *ACS Nano*, vol. 5, no. 4, pp. 3204–3213, 2011.

[7] Z. M. M. V. Yigit, A. Moore, “Magnetic nanoparticles for cancer diagnosis and therapy,” *Pharm Res.*, vol. 29, no. 5, pp. 1180–1188, 2012.

[8] S. Tong, S. Hou, B. Ren, Z. Zheng, and G. Bao, “Self-assembly of phospholipid-PEG coating on nanoparticles through dual solvent exchange,” *Nano Lett.*, vol. 11, no. 9, pp. 3720–3726, 2011.

[9] D. Guin, S. V. Manorama, S. Radha, and A. K. Nigam, “One-pot size and shape controlled synthesis of DMSO capped iron oxide nanoparticles,” *Bull. Mater. Sci.*, vol. 29, no. 6, pp. 617–621, 2006.

[10] J. Xie, S. Peng, N. Brower, N. Pourmand, S. X. Wang, and S. Sun, “One-pot synthesis of monodisperse iron oxide nanoparticles for potential biomedical applications,” *Pure*

Appl. Chem., vol. 78, no. 5, pp. 1003–1014, 2006.

[11] M. Mahmoudi, S. Sant, B. Wang, S. Laurent, and T. Sen, "Superparamagnetic iron oxide nanoparticles (SPIONs): Development, surface modification and applications in chemotherapy," *Adv. Drug Deliv. Rev.*, vol. 63, no. 1–2, pp. 24–46, 2011.

[12] E. Lim, Y. Huh, J. Yang, K. Lee, and J. Suh, "pH-Triggered Drug-Releasing Magnetic Nanoparticles for Cancer Therapy Guided by Molecular Imaging by MRI," *Adv. Mater.*, vol. 23, pp. 2436–2442, 2011.

[13] D. Destouches *et al.*, "A simple approach to cancer therapy afforded by multivalent pseudopeptides that target cell-surface nucleoproteins," *Cancer Res.*, vol. 71, no. 9, pp. 3296–3305, 2011.

[14] J. B. Haun, N. K. Devaraj, S. a Hilderbrand, H. Lee, and R. Weissleder, "Bioorthogonal chemistry amplifies nanoparticle binding and enhances the sensitivity of cell detection.," *Nat. Nanotechnol.*, vol. 5, no. 9, pp. 660–665, 2010.

[15] A. Hofmann *et al.*, "Highly monodisperse water-dispersable iron oxide nanoparticles for biomedical applications," *J. Mater. Chem.*, vol. 20, pp. 7842–7853, 2010.

[16] R. Jelinek *et al.*, "Polydiacetylenes – recent molecular advances and applications," *RSC Adv.*, vol. 3, no. 44, p. 21192, 2013.

[17] J. A. Dong and J. M. Kim, "Fluorogenic polydiacetylene supramolecules: Immobilization, micropatterning, and application to label-free chemosensors," *Acc. Chem. Res.*, vol. 41, no. 7, pp. 805–816, 2008.

[18] O. Yarimaga, J. Jaworski, B. Yoon, and J.-M. Kim, "Polydiacetylenes: supramolecular smart materials with a structural hierarchy for sensing, imaging and display applications," *Chem. Commun.*, vol. 48, no. 19, p. 2469, 2012.

[19] J. H. Fang *et al.*, "Dual-Targeting Lactoferrin-Conjugated Polymerized Magnetic Polydiacetylene-Assembled Nanocarriers with Self-Responsive Fluorescence/Magnetic Resonance Imaging for In Vivo Brain Tumor Therapy," *Adv. Healthc. Mater.*, vol. 5, no. 6, pp. 688–695, 2016.

[20] S. Sharma, M. Khawaja, M. K. Ram, D. Y. Goswami, and E. Stefanakos, "Characterization of 10,12-pentacosadiynoic acid Langmuir-Blodgett monolayers and their use in metal-insulator-metal tunnel devices," *Beilstein J. Nanotechnol.*, vol. 5, no. 1, pp. 2240–2247, 2014.

[21] "10,12-Heptacosadiynoic Acid 67071-94-7 _ TCI America." .

[22] T. Z. C. Viscometer and S. A. D, "Instructions for the use of," p. 98.

[23] "Thermo Fisher Scientific - Amine-Reactive Crosslinker Chemistry." 2016.

[24] L. L. Stookey, "Ferrozine---a new spectrophotometric reagent for iron," *Anal. Chem.*, vol. 42, no. 7, pp. 779–781, 1970.

[25] M. Instruments, "Inform White Paper Dynamic Light Scattering," *Malvern Guid.*, pp. 1–6, 2011.

[26] D. L. Scattering, U. Nobbmann, N. S. Characterization, Z. Nano, and M. Zetasizer, "Tips & Tricks for Nanoparticle Characterization," no. November, 2014.

[27] Malvern ZetaSizer, "Malvern Zetasizer SZ User Manual," pp. 2–15, 2013.

[28] Thermofisher, "Nanodrop 2000," 2000.

[29] W. Wu, Q. He, and C. Jiang, "Magnetic iron oxide nanoparticles: Synthesis and surface functionalization strategies," *Nanoscale Res. Lett.*, vol. 3, no. 11, pp. 397–415, 2008.

APPENDIX:

Data results the three best experiments for purchased 10 nm and 20 nm cores for unconcentrated and concentrated samples for small, medium, and large sizes of different amounts of HCDA.

Core Type	HCDA concentration (mg)	Unconc. (small sizing)	Conc. (small sizing)	Unconc. (medium sizing)	Conc. (medium sizing)	Unconc. (large sizing)	Conc. (large sizing)	Yield	Absorbance (unconc.)	Absorbance (conc.)
10 nm purchased cores	3	31.91	32.71	109.10	102.90	184.40	190.40	19.70%	0.086	0.296
		25.67	22.79	101.10	102.50	199.30	192.90	17.20%	0.086	0.182
		37.06	43.38	104.60	114.10	195.90	204.00	36.40%	0.118	0.345
Avg.		31.55	32.96	104.93	106.50	193.20	195.77			
Std. dev.		5.70	10.30	4.01	6.58	7.81	7.24			
Number of samples used		3	3	3	3	3	3			
Std. error		3.29	5.95	2.32	3.80	4.51	4.18			
10 nm purchased cores	5	32.68	29.97	111.50	101.10	195.40	193.20	31.20%	0.054	0.190
		42.24	26.43	110.40	79.19	216.20	196.30	25.80%	0.187	0.185
		31.77	27.28	92.89	87.72	207.00	214.70	43.90%	0.242	0.776
Avg.		35.56	27.89	104.93	89.34	206.20	201.40			
Std. dev.		5.80	1.85	10.44	11.04	10.42	11.62			
Number of samples used		3	2	3	2	2	2			
Std. error		3.35	1.31	6.03	7.81	7.37	8.22			
10 nm purchased cores	10	22.25	24.44	95.53	92.98	181.90	181.10	21.20%	0.123	0.236
		24.66	30.84	90.81	113.00	178.40	184.40	19.50%	0.320	0.408
		24.30	27.68	90.45	99.58	204.40	197.00	38.10%	0.178	0.327
Avg.		23.74	27.65	92.26	101.85	188.23	187.50			
Std. dev.		1.30	3.20	2.83	10.20	14.11	8.39			
Number of samples used		2	3	3	2	3	3			
Std. error		0.92	1.85	1.64	7.21	8.15	4.84			
20 nm purchased cores	3	23.85	33.76	109.10	111.00	190.50	194.30	22.10%	0.056	0.148
		23.51	29.11	84.01	95.05	181.40	192.20	26.90%	0.086	0.102
		23.62	31.08	96.32	81.72	185.20	211.70	25.80%	0.063	0.293
Avg.		23.66	31.32	96.48	95.92	185.70	199.40			
Std. dev.		0.17	2.33	12.55	14.66	4.57	10.70			
Number of samples used		2	3	3	3	3	3			
Std. error		0.12	1.35	7.24	8.46	2.64	6.18			
20 nm purchased cores	5	26.80	22.91	83.17	101.60	197.60	202.00	26.30%	0.189	0.395
		30.76	30.12	69.95	82.90	214.50	209.00	14.40%	0.178	0.307
		21.62	27.04	88.04	121.10	208.20	198.90	23.40%	0.217	0.429

Avg.		26.39	26.69	80.39	101.87	206.77	203.30			
Std. dev.		4.58	3.62	9.36	19.10	8.54	5.17			
Number of samples used		2	2	3	2	2	2			
Std. error		3.24	2.56	5.40	13.51	6.04	3.66			
20 nm purchased cores	10	24.50	34.09	112.90	92.67	193.30	189.80	15.30%	0.259	0.471
		22.21	30.20	90.63	86.71	189.70	193.70	30.30%	0.275	0.678
		32.75	26.20	108.00	93.83	193.00	193.50	38.10%	0.291	0.383
Avg.		26.49	30.16	103.84	91.07	192.00	192.33			
Std. dev.		5.54	3.95	11.70	3.82	2.00	2.20			
Number of samples used		3	2	3	3	3	3			
Std. error		3.20	2.79	6.76	2.21	1.15	1.27			

Data results the three best experiments for purchased 20 nm cores only for unconcentrated and concentrated samples for small, medium, and large sizes of different amounts of PCDA.

Core Type	PCDA concentration (mg)	Unconc. (small sizing)	Conc. (small sizing)	Unconc. (medium sizing)	Conc. (medium sizing)	Unconc. (large sizing)	Conc. (large sizing)	Yield	Absorbance (unconc.)	Absorbance (conc.)
20 nm purchased cores	3	41.70	42.87	63.17	50.71	218.90	233.20	13.40%	0.149	0.307
		37.23	42.53	51.04	78.00	257.90	250.70	10.20%	0.144	0.437
		46.66	43.60	51.32	52.51	258.10	250.80			
Avg.		41.86	43.00	55.18	60.41	244.97	244.90			
Std. dev.		4.72	0.55	6.92	15.26	22.57	10.13			
Number of samples used		2	2	2	2	3	3			
Std. error		3.34	0.39	4.90	10.79	13.03	5.85			
20 nm purchased cores	5	29.33	39.54	52.16	134.90	238.20	233.10	15.30%	0.282	0.443
		40.10	50.23	52.38	83.70	236.90	238.50	12.50%	0.227	0.522
		33.46	49.75	44.27	125.10	247.80	227.00	20.70%	0.214	0.590
Avg.		34.30	46.51	49.60	114.57	240.97	232.87			
Std. dev.		5.43	6.04	4.62	27.18	5.95	5.75			
Number of samples used		3	2	2	3	3	3			
Std. error		3.14	4.27	3.27	15.69	3.44	3.32			
20 nm purchased cores	10	36.64	34.88	117.20	54.33	238.20	239.60	18.30%	0.502	0.809
		35.59	37.18	109.60	92.84	245.20	227.30	18.10%	0.462	0.769
		41.18	33.44	163.40	109.60	255.30	255.60	26.80%	0.251	0.697
Avg.		37.80	35.17	130.07	85.59	246.23	240.83			
Std. dev.		2.97	1.89	29.12	28.34	8.60	14.19			

Number of samples used		3	3	3	2	2	3			
Std. error		**1.72**	**1.09**	**16.81**	**20.04**	**6.08**	**8.19**			

CALCULATIONS:

How to calculate volume of cores:

(taken from previous master student in this project)

2 mmol $Fe(acac)_3$ is the starting reactant

Balance equation: 3 mmol $Fe(acac)_3$ + …. → Fe_3O_4

2 mmol $Fe(acac)_3$ x (1 mmol Fe_3O_4/ 1 mmol $Fe(acac)_3$) = 2/3 mmol Fe_3O_4

2/3 mmol Fe_3O_4 x 1 mol/1000 mmol x 231.533 g/mol Fe_3O_4 = 0.15436 g Fe_3O_4

MNP concentration in hexane: 0.15436 g Fe_3O_4 / 10 ml of hexane = 0.0154 g/ml iron oxide in hexane

What we want: 100µg in flask because 100µg/ml solution for this procedure

3 flasks → 0.3 mg cores

0.3 mg (1g/1000mg) (1 ml/0.0154 g) (1000µL/1mL) = 19.5 µL of iron cores = ~ 20 µL of iron cores

Ferrozine Standard:

MNP stock solution: 100µg/ml solution of MNPs in toluene

20 µL of cores = 0.020 mL

0.020 mL (5mg/mL) = 0.1 mg MNP cores in toluene → 0.033 mg MNPs in each flask in toluene if there are a total of 3 flasks

Standard curves:

Use $C_1V_1 = C_2V_2$

20 µL of cores to have 0.1 mg/mL solution (100%)

If 15 mL is the 20% DMSO solution desired volume, then…

0.1 mg/15 mL → 100% → 0.0067 mg/mL
0.09 mg/15 mL → 90% → 0.006 mg/mL
0.08 mg/15 mL → 80% → 0.0053 mg/mL
0.07 mg/15 mL → 70% → 0.0047 mg/mL
0.06 mg/15 mL → 60% → 0.004 mg/mL
0.05 mg/15 mL → 50% → 0.0033 mg/mL

0.04 mg/15 mL → 40% → 0.0027 mg/mL
0.03 mg/15 mL → 30% → 0.002 mg/mL
0.02 mg/15 mL → 20% → 0.0013 mg/mL
0.01 mg/15 mL → 10% → 0.00067 mg/mL

(20 µL of cores / t) (0.1 mg/ml) = 0.0067 mg/ml → t = 299 µL of total solution
20 µL → Add 279 µL of toluene → 299 µL (0.0067 mg/ml) → 100%

(299 µL/ t) (0.0067 mg/ml) = 0.006 mg/ml → t = 334 µL of total
299 µL → Add 35 µL of toluene → 334 µL (0.006mg/ml) → 90%

(334 µL/ t) (0.006 mg/ml) = 0.0053 mg/ml → t = 378 µLof total
334 µL → Add 44 µL of toluene → 378 µL (0.0053 mg/ml) → 80%

(378 µL/ t) (0.0053 mg/ml) = 0.0047 mg/ml → t = 426 µL total
378 µL → Add 48 µL of toluene → 426 µL (0.0047 mg/ml) → 70%

(426 µL / t) (0.0047 mg/ml) = 0.004 mg/ml → t = 501 µLtotal
426 µL→ Add 75 µL of toluene → 501 µL (0.004 mg/ml) → 60%

(501 µL /t) (0.004 mg/ml) = 0.0033 mg/ml → t = 607 µL total
501 µL → Add 106 µL of toluene → 607 µL (0.0033 mg/ml) → 50%

(607 µL/ t) (0.0033 mg/ml) = 0.0027 mg/ml → t = 742 µL total
607 µL → Add 135 µL of toluene → 742 µL (0.0027 mg/ml) → 40%

(742 µL/ t) (0.0027 mg/ml) = 0.002 mg/ml → t = 1002 µL total
742 µL → Add 260 µL of toluene → 1002 µL (0.002 mg/ml) → 30%

(1002 µL/ t) (0.002 mg/ml) = 0.0013 mg/ml → t = 1542 µL total
1002 µL → Add 540 µL of toluene → 1542 µL (0.0013 mg/ml) → 20%

(1542 µL/ t) (0.0013 mg/ml) = 0.00067 mg/ml → t = 2992 µL total
1542 µL → Add 1450 µL of toluene → 2992 µL (0.00067 mg/ml) → 10%

Standard curves were made by dissolving the desired cores in toluene to make different concentration solutions. These curves were then used to determine the percent yield assay using a ferrozine assay, in which water was used as a control and ferrozine as the experiment to gain absorbance values at 562 nm and 810 nm.

Standard curve for purchased 10 nm cores:

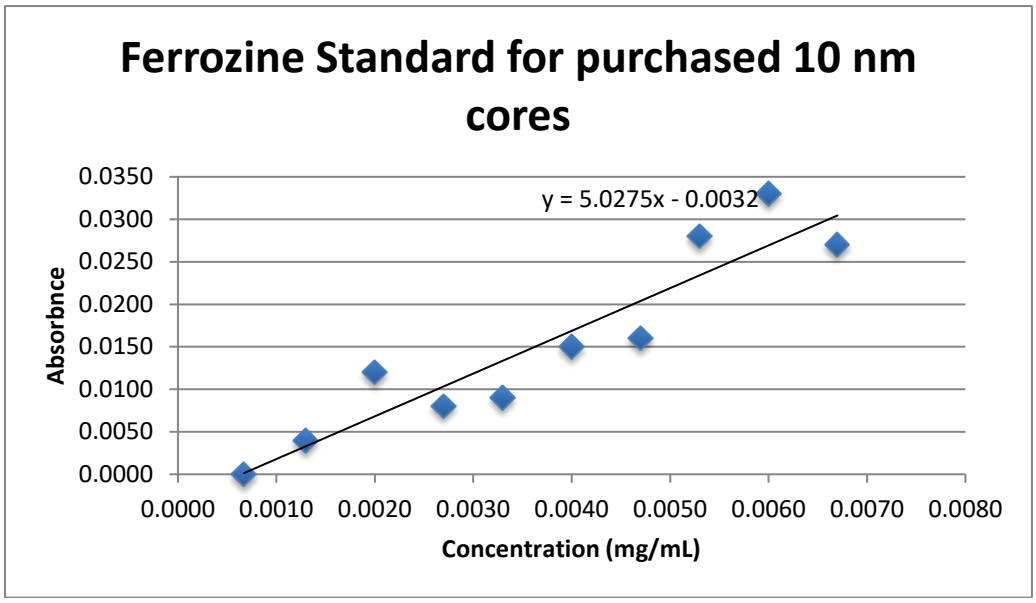

Standard curve for purchased 20 nm cores: